

## Stability Analysis of Composite Panels with Stiffeners and Circular Cutouts

Husam Al-Qablan <sup>1)✉</sup>, Hazim Dwairi <sup>1)</sup>, Nasim Shatarat <sup>1)</sup>, Taleb Rosan <sup>1)</sup> and Tamara Al-Qablan <sup>2)</sup>

<sup>1)</sup> Department of Civil Engineering, Hashemite University, 13115 Zarqa, Jordan

✉ Corresponding author. Tel: +962 (5) 3903333 EXT 4708; Fax: +962 (5) 3826613

E-mail address: hqablan@hotmail.com

<sup>2)</sup> Department of Information Technology, Al-Huson University College, Al-Balqa Applied University, 50 Al-Huson, Jordan

### ABSTRACT

Buckling of simply supported square orthotropic plates with multi-blade stiffeners is addressed herein. An approximate, semi-analytical model for such plates subjected to in-plane loading is derived. The optimal buckling load of simply supported laminated composite blade-stiffened panels with circular cutouts is predicted using Finite Element Analysis. In this optimization, the design variables were the cutout size, cutout location, fiber orientation angles, number and locations of stiffeners. Three types of in-plane loading were considered; namely, uniaxial, biaxial and shear loading. Based on the model studies, the total increase in the buckling load due to the presence of cutouts and stiffeners can reach up to 5 times in uniaxial loading, 7 times in biaxial loading and 2 times in shear loading compared to perfect plates. Several other imperative findings are identified based upon the various parameters influencing the buckling behavior. Guidelines for the optimal stiffeners' configurations and cutouts' proportioning are developed.

**KEYWORDS:** Buckling, Stiffened panels, Cutouts, FE analysis, Composite structures.

### INTRODUCTION

Linear plate buckling is an important issue in designing many structural systems, particularly when minimum weight is a primary design objective. Cutouts in composite laminated panels are often found for accessibility reasons or to just lighten the structure. In aircraft wings, for example, cutouts are needed for fuel lines, electric lines or to reduce the overall weight of the wing. The presence of these cutouts complicates the stress distribution in the composite panels. The effects of cutouts in laminated plates subjected to different work load conditions on the buckling loads have been investigated by many researchers over the past years

(Ghannadpour et al., 2006; Jain and Kumar, 2004; Anil et al., 2007; Kong et al., 2001; Larsson, 1987). They concluded that buckling load decreases as the central circular/elliptical/square hole dimensions increase.

Stiffeners have been widely used in the composite laminated panels to overcome the reduction in the buckling load due to the presence of cutouts in the composite laminated panels. A great deal of attention has been focused on plates reinforced by stiffeners to improve their buckling behavior. Many researchers used numerical methods like FEM to clearly understand the buckling behavior of composite panels (Kolakowski and Kubiak, 2005; Kim, 1996). Kang and Kim (2005), Perry et al. (1997) and Bisagni and Lanzi (2002) studied the buckling and postbuckling behavior of composite stiffened panels subjected to compressively axial loads. In their studies, optimization techniques were applied to

nonlinear finite element analysis codes. The optimization aimed at minimizing the weight of stiffened composite structures under load constrains in the postbuckling region.

Analysis of laminated composite stiffened panels is complex. Many researchers have tried to develop some guidelines and curves, which would be helpful for the designers (Nemeth, 1997; Pecce and Cosenza, 2000; Iyengar and Chakraborty, 2004). Alinia (2005) studied the buckling behavior of stiffened plates subjected to shear loads. In his study, over 1200 plates were analyzed to study the role stiffened and to come up with some limits for an optimization design procedure. Mallela and Upadhyay (2006) presented some parametric studies on simply supported laminated composite blade-stiffened panels subjected to shear loads. They concluded that panels with high orthotropy ratio and less pitch length (more number of stiffeners with less depth) are preferable for shear buckling point of view.

This study is mainly concerned with the buckling behavior of simply supported orthotropic and laminated composite blade-stiffened panels with circular cutouts subjected to three types of loading; uniaxial, biaxial and shear loading. The weights for all composite laminated plates were kept constant to achieve the optimal buckling load. The effects of the circular cutouts and the blade-stiffeners on the buckling behavior of laminated composite plates were taken into consideration. Based on the analysis, few important parameters influencing the buckling behavior are identified and guidelines for better stiffeners and cutouts' proportioning are

developed, which will be helpful for the designers.

## BASIC EQUATIONS AND PROBLEM FORMULATION

The elastic buckling load of a perfect square orthotropic stiffened panel is computed using Rayleigh-Ritz method. The assumed displacement field, which satisfies the boundary condition of a simply supported plate, is given by the form of Fourier series:

$$w = \sum_{m=1}^{\infty} \sum_{n=1}^{\infty} \left( q_{mn} \sin\left(\frac{m\pi x}{a}\right) \sin\left(\frac{n\pi y}{b}\right) \right) \quad (1)$$

$$\text{@ } x = 0; x = a : w = 0, M_x = 0 \text{ or } \left( \frac{\partial^2 w}{\partial x^2} = 0 \right)$$

$$\text{@ } y = 0; y = b : w = 0, M_y = 0 \text{ or } \left( \frac{\partial^2 w}{\partial y^2} = 0 \right)$$

where the unknown coefficients  $q_{mn}$  represent generalized displacement amplitudes, the constants  $a$  and  $b$  are the plate length and width, respectively. The first eigenvalue (the lowest critical load) for square stiffened orthotropic plates would occur for  $m = n = 1$ ; therefore the assumed displacement field will reduce to:

$$w = q_{11} \sin\left(\frac{\pi x}{a}\right) \sin\left(\frac{\pi y}{b}\right) \quad (2)$$

According to the principle of conservation of energy, the potential energy of the orthotropic plate is defined as  $\Pi = U_1 + W_1$ , where  $U_1$  is the strain energy and  $W_1$  is the potential energy of the external loads and can be written in the forms below.

$$U_1 = \frac{1}{2} \int_0^b \int_0^a \left( D_{11} (\partial_{x,x} w)^2 + 2D_{12} (\partial_{x,x} w \partial_{y,y} w) + D_{22} (\partial_{y,y} w)^2 + 4D_s (\partial_{x,y} w)^2 \right) dx dy \quad (3)$$

$$W_1 = -\frac{1}{2} \int_0^b \int_0^a \left( N_x (\partial_x w)^2 + N_y (\partial_y w)^2 + N_{xy} (\partial_x w \partial_y w) \right) dx dy \quad (4)$$

where, the subscripts preceded by a comma denote partial derivatives (e.g.,  $\partial_{x,x} w = \frac{\partial^2 w}{\partial x^2}$ ),  $N_x$ ,  $N_y$

and  $N_{xy}$  are the internal forces acting in the middle surface of the plate due to the applied in-plane loading,  $D_{11}$ ,  $D_{22}$ ,  $D_{12}$  and  $D_s$  are the flexural and torsional

rigidities of an orthotropic plate, respectively, and are given as:

$$D_{11} = \frac{E_1}{1-\nu_1\nu_2} \frac{h^3}{12}; D_{22} = \frac{E_2}{1-\nu_1\nu_2} \frac{h^3}{12};$$

$$D_{12} = \frac{E_1\nu_2}{1-\nu_1\nu_2} \frac{h^3}{12}; D_s = \frac{Gh^3}{12}; \nu_2 = \nu_1 \frac{E_2}{E_1}$$

Herein,  $E_1, E_2, \nu_1, \nu_2$  and  $G$  are assumed to be elastic constants of an orthotropic material, i.e.,  $E_1, E_2$ ; and  $\nu_1, \nu_2$  are the moduli of elasticity and Poisson's ratios in the x and y directions, respectively.  $G$  is the shear modulus and  $h$  is the plate thickness.

For biaxial case, the load in the y direction  $N_y$  can be simplified as a function of the load in the x direction  $N_x = \mu N_x$ , where  $\mu$  is a constant ( $0 \leq \mu \leq 1$ ). The first variation of the potential energy  $\Pi$  yields the equilibrium state, and by setting the variation in the total potential energy equal to zero  $\partial_{q_{11}} \Pi = 0$ , the critical buckling load for orthotropic plate subjected to uniaxial or biaxial loads can be expressed as follows.

$$N_x = \frac{h^3 \pi^2 (4G(\nu_1\nu_2 - 1) - (1 + 2\nu_2)E_1 - E_2)}{12b^2(\nu_1\nu_2 - 1)(1 + \mu)} \quad (5)$$

For the case of orthotropic panels with blade isotropic stiffeners, two modes of buckling are usually considered; the local buckling of the plate between the stiffeners and the overall buckling (primary buckling) of the plate-stiffener combination. Herein, the derivation of buckling load is concerned with the primary buckling. The assumed displacement field for the stiffeners is given by the form of Fourier series:

$$w_{sx} = \sum_{i=1}^j q_{11} \sin\left(\frac{\pi x}{a}\right) \sin\left(\frac{\pi c_i}{b}\right) \quad (6)$$

$$w_{sy} = \sum_{i=1}^k q_{11} \sin\left(\frac{\pi d_i}{a}\right) \sin\left(\frac{\pi y}{b}\right)$$

where  $j$  and  $k$  represent the number of stiffeners parallel to the x and y direction, respectively, and  $d_i$  and  $c_i$  are the location of the stiffeners in the x and y direction, respectively. The potential energy for the orthotropic panels with blade isotropic stiffeners can be expressed as follows:

$$\Pi = U_1 + U_2 + U_3 + W_1 + W_2 + W_3 \quad (7)$$

where  $U_1, U_2$  and  $U_3$  represent the strain energy of the orthotropic plate, stiffeners in the x direction and stiffeners in the y direction, respectively, while  $W_1, W_2$  and  $W_3$  represent the potential energy of the external loads for the orthotropic plate, stiffeners in the x direction and stiffeners in the y direction, respectively. Herein,  $U_1$  and  $W_1$  are shown in equations 3 and 4, respectively, while  $U_2, W_2, U_3$  and  $W_3$  can be expressed as follows:

$$U_2 = \sum_{i=1}^j \left( \frac{EI_{xi}}{2} \int_0^a (\partial_{x,x} w_{sx})^2 dx \right) \quad (8)$$

$$W_2 = \sum_{i=1}^j \left( -\frac{N_x A_{xi}}{2h} \int_0^a (\partial_x w_{sx})^2 dx \right) \quad (9)$$

$$U_3 = \sum_{i=1}^k \left( \frac{EI_{yi}}{2} \int_0^b (\partial_{y,y} w_{sy})^2 dy \right) \quad (10)$$

$$W_3 = \sum_{i=1}^k \left( -\frac{N_y A_{yi}}{2h} \int_0^b (\partial_y w_{sy})^2 dy \right) \quad (11)$$

Substituting equations 3, 4, 8, 9, 10 and 11 into equation 7 and differentiating with respect to the coefficient  $q_{11}$  and by setting the variation in the total potential energy equal to zero  $\partial_{q_{11}} \Pi = 0$ , the critical buckling load for orthotropic plate with multi-blade isotropic stiffeners subjected to uniaxial or biaxial loads can be expressed as follows:

$$N_x = \frac{\left[ -\frac{h^3((1+\nu_2)E_1 + (1+\nu_1)E_2)}{(\nu_1\nu_2 - 1)} + 4 \left( Gh^3 + 6D \left( \left( \sum_{i=1}^j \sin\left(\frac{\pi c_i}{b}\right) \right)^2 \sum_{i=1}^j \gamma_i + \left( \sum_{i=1}^k \sin\left(\frac{\pi d_i}{b}\right) \right)^2 \sum_{i=1}^k \lambda_i \right) \right] \pi^2}{12b^2 \left( 1 + \mu + 2 \left( \sum_{i=1}^j \sin\left(\frac{\pi c_i}{b}\right) \right)^2 \sum_{i=1}^j \delta_i + 2\mu \left( \sum_{i=1}^k \sin\left(\frac{\pi d_i}{b}\right) \right)^2 \sum_{i=1}^k \chi_i \right)} \quad (12)$$

where

$$\gamma_i = \frac{EI_{xi}}{Db}; \lambda_i = \frac{EI_{yi}}{Db}; \delta_i = \frac{A_{xi}}{bh}; \chi_i = \frac{A_{yi}}{bh}$$

$$D = \frac{E}{1-\nu^2} \frac{h^3}{12}$$

represents the stiffness of the stiffeners.  $E$  and  $\nu$  are the modulus of elasticity and

Poisson's ration of the stiffeners, respectively.

$I_{xi}$  and  $I_{yi}$  represent the moment of inertia of stiffeners parallel to the x and y direction, respectively.

$A_{xi}$  and  $A_{yi}$  represent the cross-sectional area of stiffeners parallel to the x and y direction, respectively.

For isotropic stiffened plates, equation (12) reduces to:

$$N_x = \frac{2D\pi^2 \left( 2 + \left( \sum_{i=1}^j \sin\left(\frac{\pi c_i}{b}\right) \right)^2 \sum_{i=1}^j \gamma_i + \left( \sum_{i=1}^k \sin\left(\frac{\pi D_i}{b}\right) \right)^2 \sum_{i=1}^k \lambda_i \right)}{\left( b^2 \left( 1 + \mu + 2 \left( \sum_{i=1}^j \sin\left(\frac{\pi c_i}{b}\right) \right)^2 \sum_{i=1}^j \delta_i + 2\mu \left( \sum_{i=1}^k \sin\left(\frac{\pi D_i}{b}\right) \right)^2 \sum_{i=1}^k \chi_i \right) \right)} \quad (13)$$

**Table (1): Material properties of the lamina**

Mechanical Properties	Values
$E_1$	130.0 GPa
$E_2$	10.0 GPa
$E_3$	10.0 GPa
$G_{12} = G_{13}$	5.0 GPa
$\nu_{12} = \nu_{13}$	0.35
$\nu_{23} = \nu_{32}$	0.35

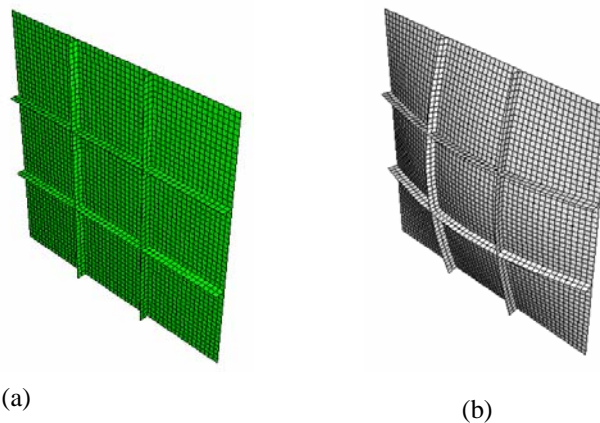


**Figure (1): Orthotropic blade-stiffened panel (a) before buckling (b) after buckling**

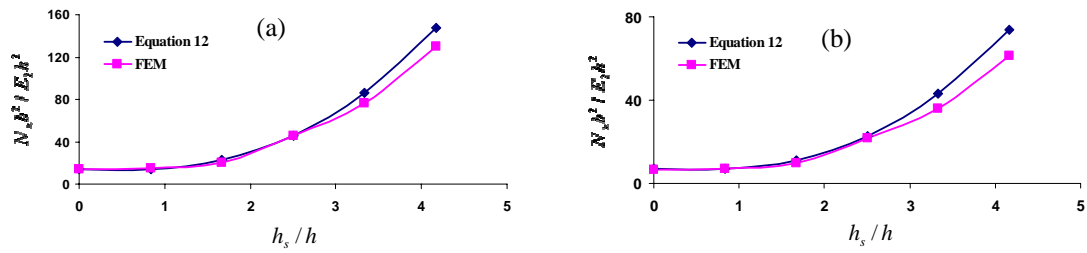


Figure (2): Nondimensional buckling load for orthotropic blade-stiffened panels subjected to (a) uniaxial loads (b) biaxial loads

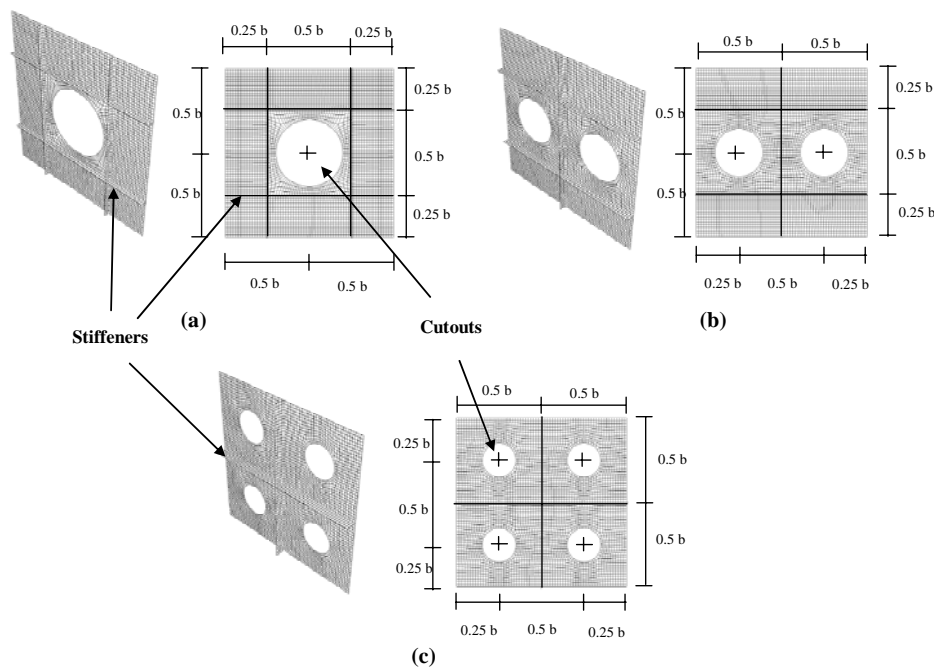


Figure (3): Undeformed shape for the laminated composite blade-stiffened panels with circular cutouts (a) case 1 (b) case 2 (c) case 3

**VALIDATION**

The present model described in the previous section was incorporated into a MATHEMATICA software, and computed results have been compared with finite element analysis using ABAQUS software for a variety of plates and stiffener dimensions. Herein, results are limited to orthotropic panels with isotropic stiffeners.

The plate dimension is 1000 mm x 1000 mm. The thickness of the plate and the stiffeners is  $t = 12mm$ . The material properties of the orthotropic plate are given in Table 1. The adopted elastic material properties for the isotropic stiffeners in each computation are Young's modulus  $E = 130 GPa$  and Poisson's ratio  $\nu = 0.35$ . In this comparison, two equally spaced

stiffeners in each direction with different heights  $h_s$  were used to compute the critical loads for the uniaxial and biaxial cases as shown in Figure 1. The finite element model is composed of mainly four noded quadrilaterals, stress/displacement shell element with reduced integration and large-strain formulation

(ABAQUS manual). Each node has six degrees of freedom. The orthotropic stiffened panels are divided into a sufficient number of elements to allow for free development of buckling modes and displacements. Some trial runs are also carried out to study the convergence of the results.

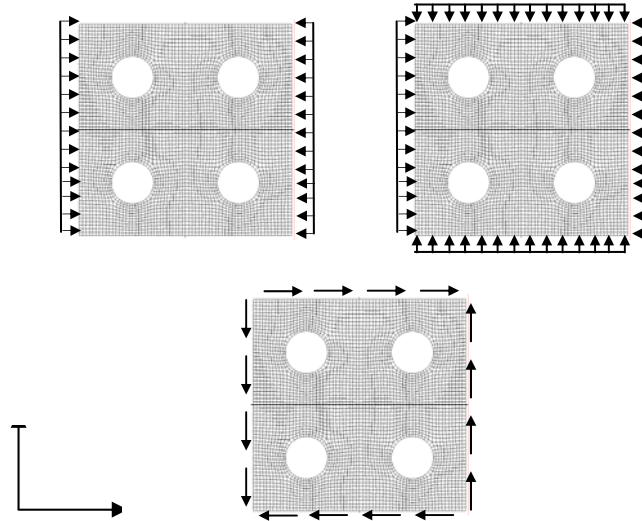


**Figure (4): Loading system (a) uniaxial loading (b) biaxial loading (c) shear loading**

The results of uniaxial and biaxial load cases are compared to finite element results as shown in Figure 2. From these results, it can be observed that the present model and finite element results are in good agreement. It is worth mentioning that the comparison between theoretical and numerical values shown in Figure 2 reveals some notable discrepancies, mainly with the deeper stiffeners. This is mainly due to the effect of the torsional stiffness and shear deformation accounted for in the finite element model, but not in the present model. This explains most of the marginal differences between these two curves.

#### **MODELING COMPOSITE LAMINATED STIFFENED PANELS WITH STIFFENERS AND CIRCULAR CUTOUTS**

Modeling composite laminated stiffened panels

needs extra attention in defining the properties of the plates, stiffeners, number of layers and fibers orientation angles of each layer. In the present work, Eigenbuckling analysis is performed for the laminated composite blade-stiffened panels using a finite element package ABAQUS. The plate dimension is also 1000 mm x 1000 mm. The thickness of each layer of this eight-layer laminates is 1.5 mm. The properties of the material of the lamina are given in Table 1. The model is composed of mainly four noded quadrilaterals, stress/displacement shell element with reduced integration and large-strain formulation. Three noded shell elements are only used in irregular zones around the holes as shown in Figure 3.

In this study, three different cases of simply supported square plates with circular cutouts and stiffeners were studied; case 1: one hole at the center of

the laminate with two stiffeners in each direction located at 0.25% and 0.75% of edge length, case 2: two holes with two stiffeners parallel to the x direction located at 25% and 0.75% of edge length and one stiffener parallel to the y direction located at 0.5% of the plate edge, case 3: four holes with one stiffener in each direction located at 0.5% of the plate edges. The locations of the holes and stiffeners for the three cases are shown in Figure 3. The plate area is located in the xy plan. For uniaxial loading, the compressive loads were applied in the x direction, while for biaxial and shear loadings, the loads were applied in the x and y directions as shown in Figure 4. Series of pre-selected

cases are modeled to verify the accuracy of the method of analysis. The results are compared to theoretical and numerical values available in the literature. Table (2) shows a comparison between the current study and theoretical results for isotropic panels without stiffeners subjected to uniaxial, biaxial and shear loads, while Table (3) shows a comparison between the current study and results available in the literature for composite laminated plate [0,90]2s with circular cutout subjected to uniaxial loads. From these results, it can be observed that the present study and the values available in the literature are in good agreement.

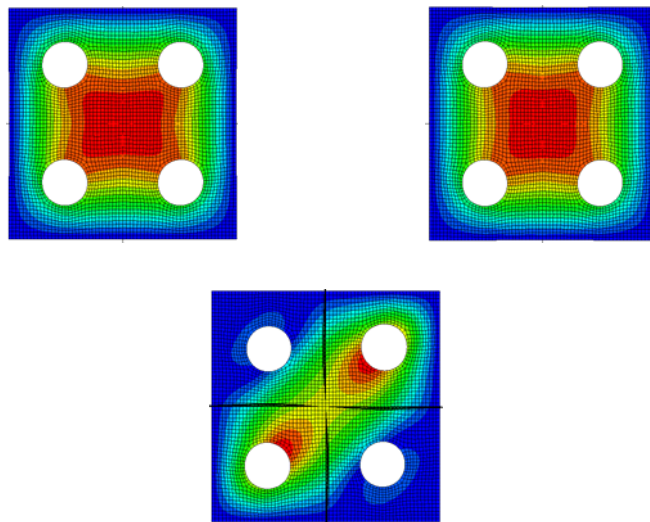


**Figure (5): First buckling mode shape for (a) uniaxial loading (b) biaxial loading (c) shear loading**

The buckling mode shapes obtained in the present study are similar in respect with the buckling mode shapes available in the literature as shown in Figure 5. In the present study, the weights for all panels were kept constant through utilizing the areas removed by circular cutouts in constructing the stiffeners. The stacking sequences, numbers and thicknesses of layers of the stiffeners are identical to that of the laminated panels. The length of each stiffener is equal to the edge length of the plate (1000 mm). The edges of the stiffeners are not penetrating the plates as shown in Figure 3. The

depths of each stiffener in the three cases are shown in Table 4.

#### **EFFECT OF CUTOUT SIZE, LOCATION AND NUMBER OF STIFFENERS ON THE BUCKLING LOADS**

In order to achieve the optimal cutout size and location, optimal fiber orientation angles and optimal number of stiffeners, the laminated panels were subjected to uniaxial, biaxial and shear loads. The ratio of the cutout diameter (d) to the plate width (b) for

plates with one hole (case 1) is varied from 0.0 to 0.8. The removed areas for plates with one hole (case 1) were divided by 2 and 4 to calculate the new areas for cutouts in plates with two holes (case 2) and plates with

four holes (case 3), respectively. These removed areas were used to construct the stiffeners in the three cases as shown in Figure 3 and Table (4).

**Table (2): Comparison of results between theoretical and numerical methods for isotropic panels without stiffeners**

Isotropic Material	E (Pa)	$\nu$	b (m)	h (m)	nondimensional buckling load (Exact) $\frac{N_{cr} b^2}{Eh^3}$	nondimensional buckling load (Numerical) $\frac{N_{cr} b^2}{Eh^3}$	Percentage difference
Uniaxial Case $N_{cr} = \frac{4\pi^2 D}{b^2}$	$2 \times 10^{11}$	0.3	1.0	0.0005	3.61524	3.6176	0.065
				0.0010	3.61524	3.6170	0.057
				0.0050	3.61524	3.6096	0.157
				0.0100	3.61524	3.59225	0.636
				0.0200	3.61524	3.55234	1.739
				0.0300	3.61524	3.51024	2.904
Biaxial Case $N_{cr} = \frac{2\pi^2 D}{b^2}$	$2 \times 10^{11}$	0.3	1.0	0.0005	1.80762	1.8088	0.065
				0.0010	1.80762	1.80865	0.057
				0.0050	1.80762	1.80476	0.158
				0.0100	1.80762	1.79613	0.636
				0.0200	1.80762	1.77617	1.739
				0.0300	1.80762	1.75513	2.903
Shear Case $N_{cr} = \frac{9.34\pi^2 D}{b^2}$	$2 \times 10^{11}$	0.3	1.0	0.0005	8.44158	8.4504	0.100
				0.0010	8.44158	8.4500	0.100
				0.0050	8.44158	8.4328	0.104
				0.0100	8.44158	8.3920	0.587
				0.0200	8.44158	8.2835	1.870
				0.0300	8.44158	8.1499	3.450

**Table (3): Comparison of results between current study and results available in the literature for composite plate [0,90]2s with circular cutout subjected to uniaxial loads**

d/b	nondimensional buckling load (Ghannadpour et al.) $\frac{N_{cr} b^2}{E_2 h^3}$	nondimensional buckling load (Numerical) $\frac{N_{cr} b^2}{E_2 h^3}$
0.0	13.79	13.60
0.1	12.80	13.07
0.2	10.82	10.53
0.3	8.97	8.80
0.4	7.51	7.42
0.5	6.39	6.40
0.6	5.63	5.31
0.8	4.43	4.37

**Table (4): Circular cutouts' and stiffeners' dimensions**

d/b	Area removed by cutouts/total area of the plate	depth of each stiffener		
		case 1	case 2	case 3
0.1	0.00785398	0.0019635	0.00261799	0.0039270
0.2	0.0314159	0.0078540	0.0104720	0.0157080
0.3	0.0706858	0.0176715	0.0235619	0.0353429
0.4	0.125664	0.0314159	0.0418879	0.0628319
0.5	0.196350	0.0490874	0.0654498	0.0981748
0.6	0.282743	0.0706858	0.0942478	0.141372
0.7	0.384845	0.0962112	0.1282817	0.192423
0.8	0.502655	0.1256638	0.1675517	0.251327

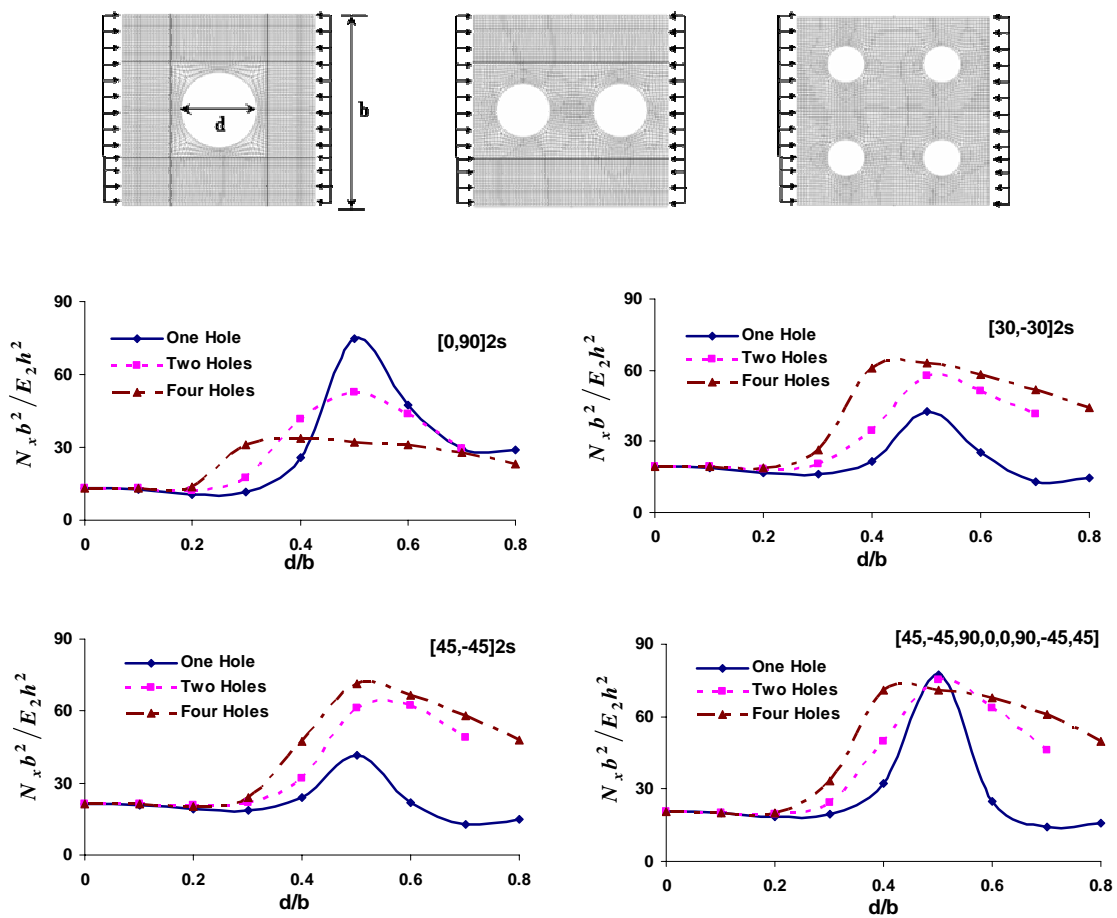


**Figure (6): Nondimensional buckling load for laminated composite blade-stiffened panels with circular cutouts subjected to uniaxial loads**

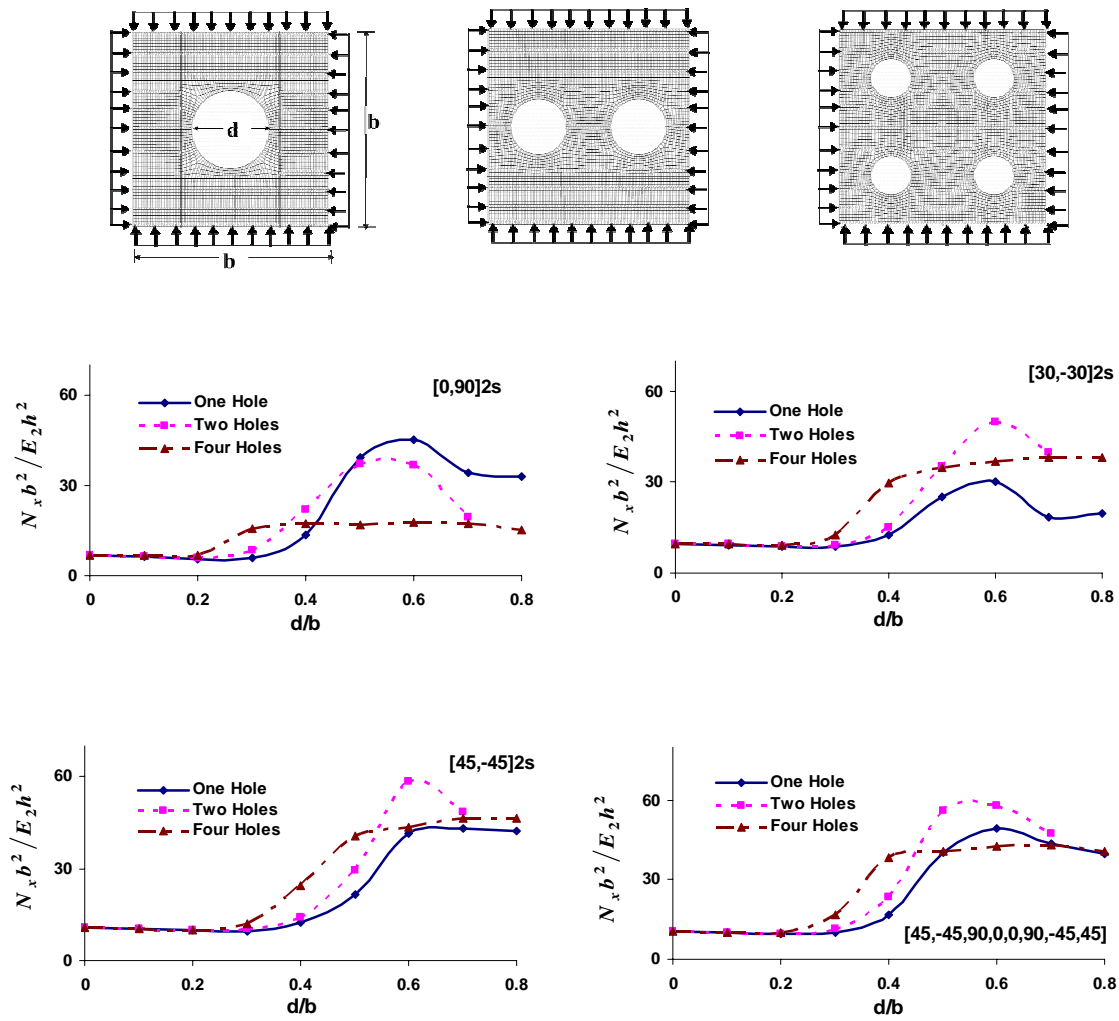


Figure (7): Nondimensional buckling load for laminated composite blade-stiffened panels with circular cutouts subjected to biaxial loads

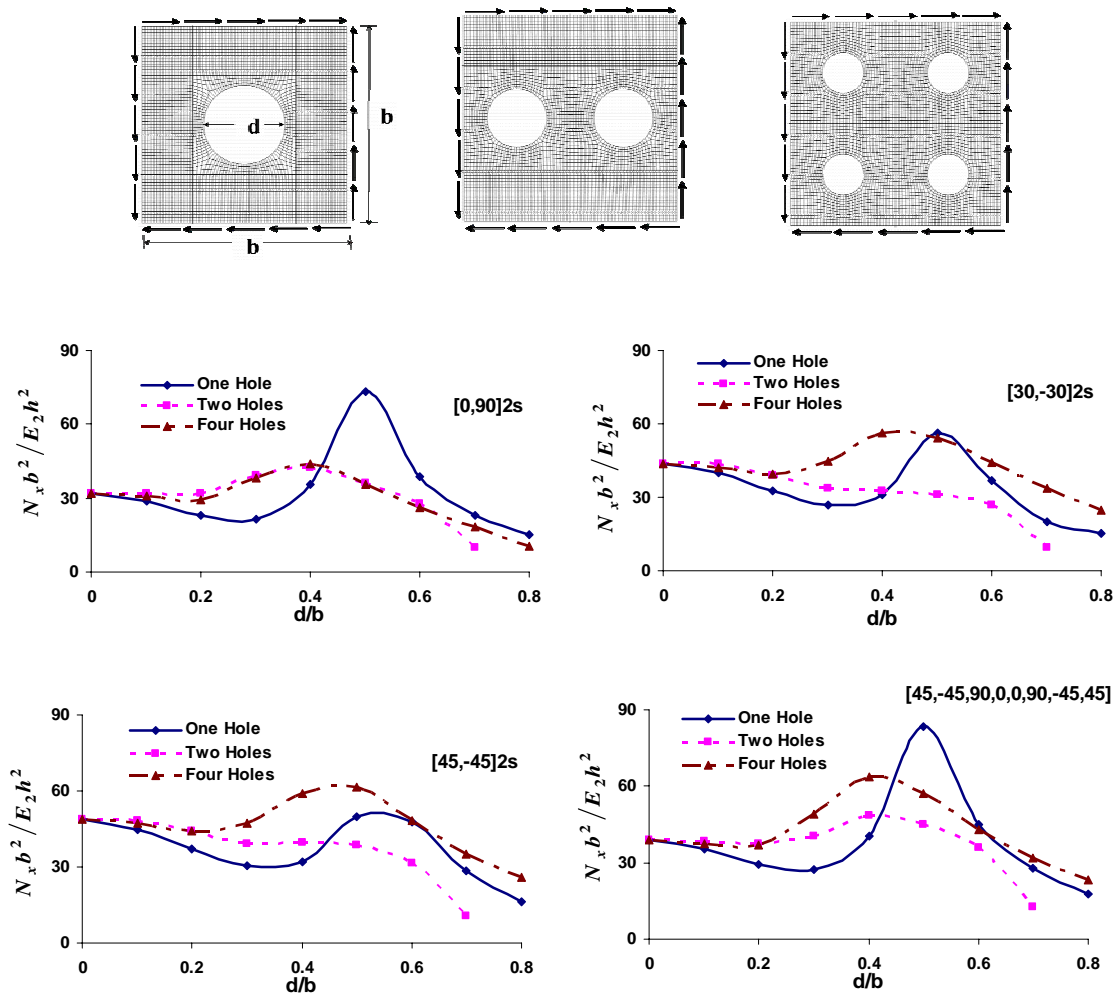


Figure (8): Nondimensional buckling load for laminated composite blade-stiffened panels with circular cutouts subjected to shear loads

It is well known that cutouts in laminated plates reduce the buckling loads (Ghannadpour et al., 2006). Also, it is well known that stiffeners in laminated plates increase the buckling loads (Mallela and Upadhyay, 2006). Herein, the interactions between the cutouts and stiffeners in laminated plates were studied to achieve the optimal buckling loads for plates having the same thicknesses and weights. For uniaxial and biaxial loading cases, Figures 6 and 7 show that the interactions between cutouts and stiffeners when changing the (d/b) ratio from 0.0 to 0.3 do not have any considerable effect

on the buckling loads compared to the perfect plate. For the (d/b) ratio from 0.4 to 0.6, it can be clearly seen from the Figures that the effect of stiffeners dominates the effect of cutouts and the total buckling load increases. The total increase in the buckling load can reach up to 5 times in uniaxial case and 7 times in biaxial case compared to the perfect plate. For the (d/b) ratio from 0.7 to 0.8, the buckling loads decrease and the effect of cutouts dominates the effect of stiffeners. The reason for this diminution in the buckling load is due to the reduction in the rigidity of the plate. The

spaces left between the cutouts became smaller and the stiffeners became larger. For these reasons, two types of buckling failure could occur; local buckling in the plate

reign (anti-symmetric mode) or local buckling in the stiffeners.

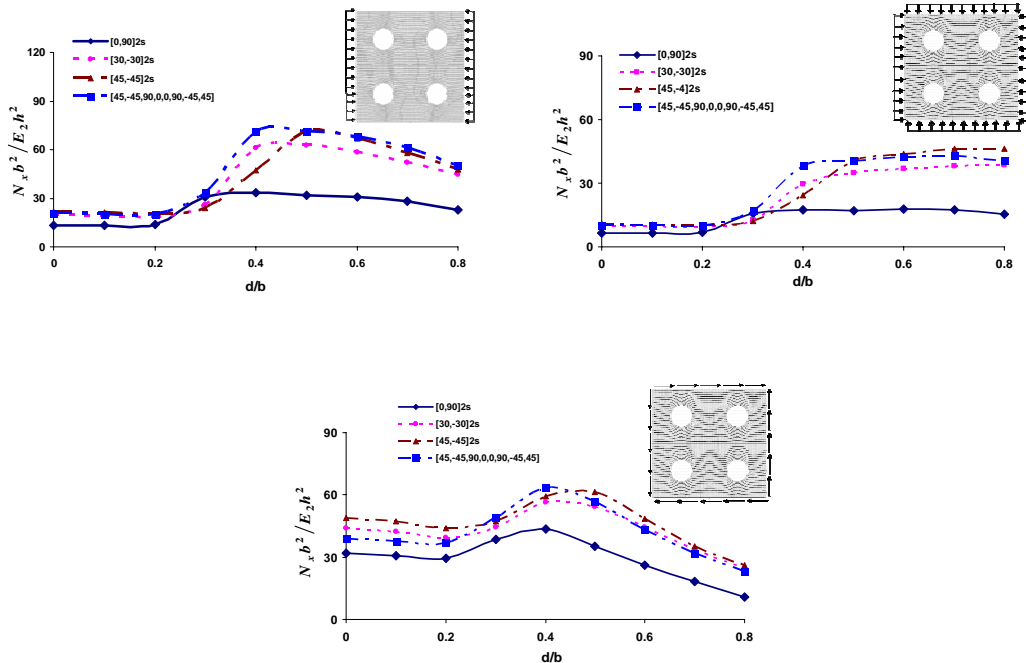


**Figure (9): Nondimensional buckling load for laminated composite blade-stiffened panels with circular cutouts subjected to (a) uniaxial loading (b) biaxial loading (c) shear loading**

For the shear loading case, it can be seen from Figure 8 that the plates are more sensitive to the cutout size. For  $(d/b)$  ratio from 0.0 to 0.3, the buckling load decreases and the effect of cutouts dominates the effect of stiffeners, while for  $(d/b)$  ratio from 0.4 to 0.6 the total buckling loads start to increase and the effect of stiffeners dominates the effect of cutouts. For  $(d/b)$  ratio from 0.7 to 0.8, the buckling loads decrease and the effect of cutouts dominates the effect of stiffeners. The total increase in the buckling load for the shear loading case can reach up to 2 times compared to the perfect plate.

The effect of fiber orientations on the buckling loads depends mainly on the cutout size, location and number of stiffeners as shown in Figures (6 - 8), the largest effect appears for  $(d/b)$  ratio from 0.4 to 0.6. Figure 9

shows the effect of fiber orientations on the buckling loads for case 3 (four holes with one stiffener in each direction) subjected to uniaxial, biaxial and shear loading. It can be clearly seen from the figure that the best performance was achieved using  $[45,-45, 90, 0, 0, 90,-45, 45]$  fiber orientations in the three loading cases.

The optimal buckling load of simply supported square laminated composite blade-stiffened panels with circular cutouts for the three cases was found for  $(d/b)$  ratio from 0.4 to 0.6. It is worth mentioning that if the percentage of cutouts  $(d/b)$  exceeds the optimal limit, the total buckling load will decrease and the effect of cutouts will dominate the effect of stiffeners. This optimum limit depends on a lot of factors such as fiber orientation, type of loading, number and location of cutouts and stiffeners.

## CONCLUSION

In the present work, the buckling behavior of square simply supported orthotropic plates with multi-blade stiffeners and laminated composite blade-stiffened panels with circular cutouts subjected to in-plane loading was investigated. The following conclusions can be drawn:

- An approximate, semi-analytical model for buckling of simply supported square orthotropic plates with multi-blade stiffeners subjected to in-plane loading is derived.
- The optimal buckling load of simply supported square laminated composite blade-stiffened panels with circular cutouts subjected to three types of loading; namely, uniaxial compression, biaxial

compression and shear loading was found for (d/b) ratio from 0.4 to 0.6.

- The total increase in the buckling load due to cutouts and stiffeners in the laminated composite panel can reach up to 5 times in uniaxial loading, 7 times in biaxial loading and 2 times in shear loading compared to the perfect plate.
- For uniaxial and biaxial load conditions, the effect of small cutouts and stiffeners (d/b ratio from 0.0 to 0.3) can be neglected.
- The buckling load is highly influenced by fiber orientation angles. The best performance was achieved using [45,-45, 90, 0, 0, 90,-45, 45] fiber orientations in the three loading cases.

## REFERENCES

- Alinia, M. 2005. A study into optimization of stiffeners in plates subjected to shear loading, *Thin-Walled Struct.*, 43: 815-845.
- Anil, V., Upadhyay, C.S. and Iyengar, N.G.R. 2007. Stability analysis of composite laminate with and without rectangular cutout under biaxial loading, *Composite Structures*, 80: 92-104.
- Bisagni, C. and Lanzi, L. 2002. Postbuckling optimization of composite stiffened panels using networks, *Composite Structures*, 58: 237-247.
- Ghannadpour, S.A.M., Najafi, A. and Mohammadi, B. 2006. On the buckling behavior of cross-ply laminated plates due to circular/elliptical cutouts, *Composite Structures*, 75: 3-6.
- HKS ABAQUS User's Manual: Theoretical Manual, ABAQUS Post Manual and Example Problem, Version 6.5.
- Iyengar, N.G.R. and Chakraborty, A. 2004. Study of interaction curves for composite laminate subjected to in-plane uniaxial and shear loading, *Composite Structures*, 64: 307-315.
- Jain, P. and Kumar, A. 2004. Postbuckling response of square laminates with a central circular/elliptical cutout, *Composite Structures*, 65: 179-185.
- Kang, J. and Kim, C. 2005. Minimum-weight design of compressively loaded composite plates and stiffeners panels for postbuckling strength by genetic algorithm, *Composite Structures*, 69: 239-246.
- Kim, K.D. 1996. Buckling behavior of composite panels using the finite elements method, *Composite Structures*, 36: 33-43.
- Kolakowski, Z. and Kubiak, T. 2005. Load-carrying capacity of thin load-walled composite structures, *Composite Structures*, 67: 417-426.
- Kong, C.W., Hong, C.S. and Kim, C.G. 2001. Postbuckling strength of composite plate with a hole, *Reinforced Plastics Compos.*, 20: 466-481.
- Larsson, P. 1987. On buckling of orthotropic compressed plates with circular holes, *Composite Structures*, 7: 102-121.
- Mallela, U. and Upadhyay, A. 2006. Buckling of laminated composite stiffened panels subjected to in-plane shear: a parametric study, *Thin-Walled Structures*, 44: 354-361.
- Nemeth, M.P. 1997. Buckling behavior of long symmetrically laminated plates subjected to shear and linearly varying axial edge loads, TP 3659: NASA.
- Pecce, M. and Cosenza, E. 2000. Local buckling curves for the design of FRR profiles, *Thin Wall Structures*, 37: 207-227.
- Perry, C.A., Gurdal, Z. and Starnes, J.H. 1997. Minimum weight design of compressively loaded stiffened panels for postbuckling response, *Engineering Optimization*, 28: 175-197.